EFDA–JET–CP(12)06/15

P.C. de Vries, A.C.C. Sips, H.T. Kim, P.J. Lomas, F. Maviglia, R. Albanese, I. Coffey, E. Joffrin, M. Lehnen, A. Manzanares, M. O'Mulane, I. Nunes, G. van Rooij, F.G. Rimini, M.F. Stamp and JET EFDA contributors

Comparison of Plasma Breakdown with a Carbon and ITER-Like Wall

Comparison of Plasma Breakdown with a Carbon and ITER-Like Wall

P.C. de Vries[1], A.C.C. Sips[2,3], H.T. Kim[4,5], P.J. Lomas[4], F. Maviglia[6], R. Albanese[6], I. Coffey[7], E. Joffrin[8], M. Lehnen[9], A. Manzanares[10], M. O'Mulane[4], I. Nunes[2,11], G. van Rooij[1], F.G. Rimini[4], M.F. Stamp[4] and JET EFDA contributors*

JET-EFDA, Culham Science Centre, OX14 3DB, Abingdon, UK

[1]FOM institute DIFFER, Association EURATOM-FOM, P.O.Box 1207, 3430BE Nieuwegein, Netherlands.
[2]European Commission, Brussels, Belgium.
[3]EFDA-CSU, Culham Science Centre, OX14 3DB, Abingdon, OXON, UK
[4]EURATOM-CCFE Fusion Association, Culham Science Centre, OX14 3DB, Abingdon, OXON, UK
[5]Department of Physics, Imperial College London, SW7 2AZ, London, UK.
[6]Associazione EURATOM-ENEA-CREATE, Univ. di Napoli Federico II, Napoli, Italy.
[7]Queen's University Belfast, BT71NN, UK.
[8]CEA-IRFM, Association Euratom-CEA , Cadarache, F-13108, France.
[9]Institut für Energie- und Klimatforschung-IEK-4, Forschungszentrum Jülich GmbH, EURATOM Association, 52425 Jülich, Germany.
[10]Laboratorio Nacional de Fusión, EURATOM-CIEMAT Association, Madrid, Spain
[11]Associação EURATOM-IST, Instituto de Plasmas e Fusão Nuclear, Lisboa, Portugal.
** See annex of F. Romanelli et al, "Overview of JET Results", (24th IAEA Fusion Energy Conference, San Diego, USA (2012)).*

Preprint of Paper to be submitted for publication in Proceedings of the
24th IAEA Fusion Energy Conference (FEC2012), San Diego, USA
8th October 2012 - 13th October 2012

ABSTRACT.
The recent installation of a full metal, ITER-like, first wall provided the opportunity to study the impact of the plasma-facing materials on plasma initiation or breakdown. This study will present for the first time a full experimental characterisation of tokamak breakdown at JET, using all discharges since 2008, covering both operations with a main chamber carbon and beryllium ITER-like wall. It was found that the avalanche phase was unaffected by the change in wall material. However, the large reduction in carbon levels resulted in significant lower radiation during the burn-through phase of the breakdown process. Breakdown failures, that usually developed with a carbon wall during the burn-through phase (especially after disruptions) were absent with the ITER-like wall. These observations match with the results obtained with a new model of plasma burn-through that includes plasma-surface interactions. The simulations show that chemical sputtering of carbon is the determining factor for the impurity content, and hence the radiation, during the burn-through phase for operations with a carbon wall. For a beryllium wall, the plasma surface effects do not raise the radiation levels much above those obtained with pure deuterium plasmas, similar as seen in the experimental study. With the ITER-like wall, operation with higher pre-fill pressures, and thus higher breakdown densities, was possible, which helped maintaining sufficient density after breakdown.

1. INTRODUCTION

The standard method to initiate plasma in a tokamak is, to ionize pre-filled gas by applying a toroidal electric field via transformer action from poloidal coils. For ITER the available electric field will limited to low values of $0.33 Vm^{-1}$, raising considerable interest to understand and optimise the breakdown phase [1]. Pre-ionization by means of microwave heating is seen as an option to provide ITER with a robust and reliable breakdown phase [2, 3, 4].

It is well-known and reported in the past that impurities have a direct impact on, both unassisted and assisted plasma breakdown phase [2, 5]. At JET un-assisted or Ohmic breakdown has previously been achieved at electric fields as low as $0.23\ Vm^{-1}$ though with Carbon-based plasma facing components [1]. The recent installation of a full metal, ITER-like, first wall [6] provided the opportunity to study directly the impact of the first wall on the breakdown characteristics. This paper will present an experimental characterisation of breakdown at JET, comparing operations with the Carbon and ITER-like wall. Here the main emphasis will be on the details in the density dynamics and impurity content.

The Ohmic breakdown process for a tokamak discharge is a complex process that can be divided into a few distinct stages. Firstly, the applied electric field initiates a classical Townsend avalanche phase, in which the main ionization process is due to collisions with electrons accelerated in the electric field [7, 2]. The collisions ensure that the average electron speed will settle at a constant value, while the ionization level, and thus the electron density and current, increases exponentially. Direct losses of electrons along the field lines will affect this phase. The distance along the field lines from the point of ionization to the wall is called the connection length which should be as long

as possible, i.e. an optimum toroidal field with small magnetic poloidal errors. Secondly, as more of the pre-fill gas is ionized, Coulomb collisions will start to dominate over atomic and molecular collisions. The electron-ion collision time is expected to exceed the electron-neutral collision time at ionization levels of roughly 5% [7, 8]. Magnetic flux surfaces can be formed when the plasma current and the associated poloidal magnetic field starts to dominate the poloidal error field, which will further improve the confinement of the particles. All the time the plasma may be expanding and comprising a larger volume. However, the plasma temperature and energy remain low due to ionization and losses from line-radiation by impurities. The plasma needs to burn-through this radiation barrier such that finally sufficient Ohmic flux can be used to further raise the current and heat the plasma, which is the final stage of the breakdown process. The burn-through phase is completed by reducing the impurity line-radiation and yielding complete ionization of the main gas.

A number of experimental breakdown studies at JET [8] or other devices [9, 2, 4, 5] have been reported in the past with recent studies focusing predominantly on assisted breakdown [10]. Characterising or diagnosing the breakdown phase of a tokamak discharge is not a straightforward task. The process is fast, at JET sometimes a few 10 of ms, and not all diagnostics may have sufficient temporal resolution for an accurate analysis. Moreover, many tokamak diagnostics are not tuned to measure the low densities, temperatures or radiation levels in the breakdown phase or only view part of the plasma. Large variations in the breakdown state, often attributed to the influence of the wall, can also complicate comparisons of a small number of discharges. The analysis strategy presented in this paper is to compare a large number of breakdowns under different conditions. All breakdown attempts at JET since 2008, covering the final period with carbon wall operations and the first phase with the ITER-like wall. This will reveal a number of relevant trends and allows a full characterization of JET breakdown providing the basis for the comparison with operations with the new ITER-like wall.

The outline of this paper will be as follows. The duration of the avalanche phase is studied in section 2. Thereafter, the development of the density during both the avalanche and burn-through phase is discussed in section 3. The influence of impurities and plasma surface interactions is shown in section 4 followed in section 5 by a comparison with a new breakdown model that includes impurities and details on plasma-surface interactions [Kim2012]. In section 6 the main conclusions will be summarised.

2. THE DURATION OF THE AVALANCHE PHASE

At JET usually two different methods are used to initiate plasma breakdown. The most common method, called Mode D, pre-magnetises the primary coil slowly with a current (usually in a range of 10 to 30kA). The vessel is pre-filled with gas and the remaining poloidal circuits are tuned such to optimise/reduce the error field in the centre of the vessel. By opening the primary circuit the current in the primary coil will decrease with the typical L/R time of the system. The change in flux through the primary coil will generate a loop voltage. Depending on pre-magnetization current it induces a loop voltage that can range from about 10V to more than 30V, i.e. electric field in the

centre of the plasma of $E(R_o) = 0.53$ and $1.6 Vm^{-1}$. The second method, called Mode B, directly ramps-up the voltage on the primary coil to values of up to about 15kV. To prevent a too early start of the breakdown a large error field is applied by the vertical field coil, which is stepped down when the required voltage has been reached, starting the avalanche process. The voltages that can be achieved with Mode B are lower than those for Mode D and in the range of 4V to 10V (i.e. $E(R_o) = 0.20$ to $0.53 Vm^{-1}$)

The breakdown process starts with what can be considered a Townsend avalanche discharge, in which the number of electrons, electron density and current increase exponentially, while the electron temperature remains very low (i.e. a few eV). This phase lasts until Coulomb collisions start to dominate and the partly ionized gas starts to behave as plasma. Traditionally the end of the avalanche phase is considered to correspond to the time when the deuterium Balmer-α (D_α) emission peaks. The time it takes to reach this stage has been estimated in ref. [2] to scale as,

$$\tau_{avalanche} \sim \frac{41}{v_{De}(\alpha - L^{-1})} \tag{1}$$

Here v_{De} is the electron drift velocity, directly proportional to E/p_{pre}, α is the first Townsend coefficient again depending on the electric field, E, and the pre-fill pressure, p_{pre}, while L represents the connection length.

Practically it is not easy to determine D_α emission peak accurately for a very large number of breakdowns at JET. Furthermore the diagnostic line-of-sight may by-pass part of the initial plasma, making the determination of time of the D_α emission peak rather ambiguous. For this study the avalanche phase duration has been determined by the time the plasma current increases from 20 to 45kA ($\tau_{20\text{-}45}$), more accurately corresponding to the characteristic current rise time. At JET the D_α emission peaks at about 30-60kA. The lower level is chosen to avoid issues with signal noise affecting the data. The avalanche time $\tau_{20\text{-}45}$ was determined for nearly all breakdowns over the period 2008-2009 (Pulse No's: range 70965-78810, in total 6392 entries). These are compared with all breakdown attempts with the new ITER-like wall in 2011-2012 (Pulse No's: range 80128-83620, in total 2793 entries). Excluded were those that use helium pre-fill or cases for which the time resolution of some key signals were not sufficient to properly monitor the short breakdown phase. Only breakdowns for which the time was allowed for the pre-fill pressure to equilibrate such that it was toroidally isobaric were included. Values for avalanche duration, $\tau_{20\text{-}45}$, vary from 2.5ms from fast Mode D breakdown to over 80ms for slower Mode B cases.

Using this breakdown database a number of trends characteristic to Townsend avalanche discharges can be shown. Through out the paper blue and green represent Mode D breakdown for the carbon and ITER-like wall data, respectively, while black and grey triangles denote Mode B cases. Failed or non-sustained breakdowns are shown by the red and orange symbols. The question is if single values of parameters such as the electric field, pre-fill pressure and the rather ambiguous connection length (or magnetic error field strength) can be used to characterise the JET avalanche phase and compared it with equation 1. Detailed studies showed that indeed the avalanche duration

is longer for cases with a higher loop voltages and magnetic fields, B_T, (i.e. longer connection lengths). Also Mode D discharges have a smaller error field compared to Mode B breakdowns. Moreover, using subsets of the database of constant B_T and E, more accurate information on the connection length can be obtained, by basically by fitting the data directly to equation 1. Using all this information one can compare the experimental values with the above equation, which is shown in figure 1.

A number of conclusions can be drawn from figure 1. In the first place, the measured data are slightly smaller than those predicted by equation 1 nevertheless the trend matches quite well over a large range of breakdown voltages, pre-fill pressures and connection lengths. It seems that especially that for, high voltage, Mode D breakdown with optimised error fields, the 0D model for a Townsend avalanche discharge works quite well. The fit breaks down, however, for lower voltage Mode B cases. The likely reason for this is an overestimation of the connection length for lower electric fields. Vessel eddy currents and currents in passive structures will vary with the applied electric field prior to plasma breakdown and thus will affect the error field (i.e. inverse connection length). If the error field is assumed to scale with the applied voltage a much improved fit could be obtained for the mode B cases. Besides error field dynamics and the influence of eddy currents, it is also possible that in these cases the 0D description fails. The plasma could expand slower and stay longer on the inside in the area providing a higher electric field and a longer connection length. A second observation is the fact that most failed breakdowns (open red symbols in figure 1) do not deviate from this scaling. It suggests that, non-sustained, breakdowns at JET are, during the avalanche phase, indistinguishable from those that can be sustained.

Finally, both the carbon and ITER-like wall data follow the same scaling indicating that the avalanche phase was little influenced by the change in wall material. The number of entries for Mode B breakdown with the ITER-like wall is spars because few attempts with an isobaric pre-fill pressure were done. More robust Mode B breakdown with the ITER-like wall was obtained with the pre-fill gas injection short before breakdown. Because in this case the pressure is not toroidally equilibrated it is difficult to assign it a single value to be used in equation 1.

3. DEVELOPMENT OF THE DENSITY AND CURRENT

When Coulomb collisions start to dominate, the partly ionized gas starts to behave like plasma. Up to that point it has mainly gained in particle and current density as the temperature remains low. Only at high enough temperatures the radiation losses due to impurity line-radiation start to reduce allowing further increases in temperature. In this section the transition to the Coulomb and burn-through phase will be discussed and the differences between burn-through with a carbon and ITER-like wall will be shown. This is done by using a specific subset of the breakdown database, consisting of only Mode D breakdown with a primary coil pre-magnetisation current in the range of 13 to 16kA, i.e. E_o~0.8V/m or V_{loop} = 12V and other poloidal coils to provide an optimum connection length. The same trends are also found for other subsets. The changes are visualised by comparing parameters at two different times, approximately at the end of the avalanche phase at t_1 = 0.031s

and thereafter at a time during the burn-through phase (when most of these entries have their peak in radiation) at $t_2 = 0.051$s. These times are specific for the loop voltage used by this subset.

In figure 2 the obtained line-integrated density (using a central vertical channel) is compared with the calculated resistivity. The latter is obtained using the plasma current signal I_p as:

$$R_p = \frac{V_{loop}}{I_p} - L_p \frac{1}{I_p} \frac{dI_p}{dt} \tag{2}$$

assuming a plasma inductance of $L_p = 4\mu$H. Two distinct characteristics are seen in figure 2a and b. For t_1, for a higher density a higher resistivity is found. During this (avalanche) phase the density develops simultaneously with the current and a higher density, thus a higher current, gives a lower resistivity (most entries have a similar loop voltage). However, later on, at t_2, the resistance scales with the density, thus inversely with the temperature, indicating the Coulomb character of the plasma. A higher density implies a lower temperature, which according to Spitzer's plasma resistivity should give a higher resistivity and a lower current. Hence, for this subset of breakdowns the transition from an atomic gas to plasma (ge. Coulomb collisions are dominating) has taken place between t_1 and t_2. The values in figure 2 can be compared with the resistance of passive conductors surrounding the plasma such as the divertor support structure (~0.75mΩ) or the JET vacuum vessel (~0.43mΩ).

From figure 2 it is also noticeable that all entries fall within a single group, suggesting that the avalanche phase does not develop differently for breakdowns with carbon plasma facing components or an ITER-like wall. The same is true for failed breakdowns. Similar observations were found in the previous section. However, slightly later, at t_2, clearly separate groups are obtained (Figure 2b). For the carbon wall entries, those that fail form a separate group above a threshold in resistance and density (i.e. too low temperature). Hardly any ITER-like wall breakdowns failed. For the same density, the resistance is lower for the ITER-like wall. This can be explained by both a lower level of impurities and a higher temperature for a given density during the burn-through phase of an ITER-like wall breakdown.

In figure 3 the density is plotted as function of the pre-fill pressure at the two times, indicating the origin of the plasma particles. Again a clear Townsend discharge characteristic is found, higher pre-fill pressure slows down the avalanche process and thus one obtains at a fix time t_1 a lower density. Looking at this graph one could argue that for very high pre-fill cases the time t_1 may be too early to characterise the final stages of the avalanche. An optimum is found and for too low pressures the density decreases again, i.e. the avalanche slows down, similar as found from equation 1. A few breakdown attempts that used too low pre-fill pressures failed during the avalanche process. These failures could be attributed to problems with the gas injection system. But all other failed entries overlay with the main group of sustained breakdowns. Again failed entries form a separate groups during the burn-through phase (at t_2).

After the avalanche phase (at t_2) the main trend is that the density (and similarly the recycling or D_α intensity) scales with the pre-fill pressure. This is especially true for the ITER-like wall breakdown and highest densities are obtained for the highest pre-fill pressures. For the carbon wall

entries, however, the scatter is larger and especially failed breakdowns gained more density than to be expected from the pre-fill. In these cases there is an additional fuelling (of electrons) likely due to wall recycling and the influx of impurities. This effect is more clearly visible if a similar analysis is done for a more robust higher voltage Mode D breakdown subset (i.e. those done to recover from deconditioning events such as disruptions) for which high burn-through densities are obtained with minimum pre-fill pressures. Unfortunately, this subset has a much smaller number of ITER-like wall entries and is therefore less suitable for the comparison presented in this paper. With the ITER-like wall it is possible and also necessary to operate with high pre-fill pressures. It is questionable if such high pre-fill pressures would have worked with the carbon wall as increasing the pre-fill and thus the density in figure 3 would have pushed it evidently into the range where it would fail. For the ITER-like wall operation with lower pre-fill was found to be more problematic as wall has the tendency to significantly pump the density after breakdown. Without additional fuelling the density with the carbon wall could maintained, while it is reduced to near zero with the ITER-like wall. It can be prevented by both a high pre-fill pressure, and thus creating a high density right after the burn-through phase, and by starting as early as possible with additional fuelling.

4. IMPURITIES AND RADIATION

Here the CIII line-intensity CII ($\lambda_{CIII} = 977Å$) at t_2 is used to characterise the level of carbon in the burn-through phase which is compared with the radiation power (P_{rad}) and line-integrated density at the same time. One should note, however, that for most entries of this data subset, the CII ($\lambda_{CII} = 904Å$) and CIII ($\lambda_{CIII} = 977Å$) line emission and radiation peak slighly before $t_2 = 0.051$s, showing that the main burn-through has already been achieved. In figure 3 it is shown that typically, for carbon wall breakdown, higher densities and radiation are obtained due to the higher levels of carbon. For the ITER-like wall the carbon levels during breakdown are significantly lower (about an order of magnitude) and the high densities are purely due to the pre-fill pressure that was used. For the ITER-like wall the radiation intensity (P_{rad}/n_e^2) is typically a factor 5 lower than with the carbon wall. The absence of any burn-through failures shows that the breakdown with the ITER-like wall is improved significantly.

Also for the ITER-like wall the dominant factor determining the radiation level during the burn-through phase was the carbon. The highest radiation intensities were mostly obtained for cases with a high carbon level. The highest level of carbon were found at the start of the operation with the new ITER-like wall, after which it decreased significantly, increasing slightly during the high power operations at the end of the experimental campaign [14].

Within the carbon data set there is a large variation in the oxygen level, which was high at the start of operations 2008 but dropped by two orders of magnitude after the first few weeks of plasma operations. However, no significant trend of breakdown with respect to the oxygen level was found and the level of carbon seems to dominate the burn-through physics. This contrasts with the impact of nitrogen which has been used in several experiments with the ITER-like wall in order to increase the divertor radiation, decreasing the target temperatures [16]. Most of the highest radiation points

with the ITER-like wall seen in figure 4 are obtained during or after N seeding experiments. There is a legacy of about two dozen discharges or one day of JET operations after the use of nitrogen has ceased.

5. Modelling of the plasma burn-through

A new model of plasma burn-through including plasma-surface interaction effects has been developed [11]. Impurity levels during the breakdown in this model are self-consistently determined by the plasma-surface interactions. These are determined via the impurity sputtering yields and it assumes an exponential decay model of the deuterium recycling coefficient. The rate and power coefficients in the Atomic Data and Analysis Structure (ADAS) package are adopted to solve energy and particle balance. Neutral screening effects are taken into account according to particle species, and the energy and particle balances are calculated. The burn-through simulations show good quantitive agreement against both carbon wall JET data [11]. In the previous sections it was shown that avalanche phase seems to be independent of the wall conditions. The simulations show that with a carbon wall the carbon content and thus the radiation builds up during the formation of the plasma due to chemical sputtering. While the model shows that physical sputtering of beryllium does not raise radiation levels much above those obtained with pure deuterium plasmas [15], similar as seen in the experimental study discussed above.

Failure of the burn-through phase is achieved if the radiation power is higher than the power obtained from Ohmic heating [Kim2012c]. Modelling showed that, for a given electric field (eg. Ohmic heating) this will occur at a specific level of pre-fill pressure. Because the radiation depends on the particle density which, as shown in figure 3b, depends on the pre-fill. Obviously, this limit is reduced for cases with higher impurity contents. Note that indeed for the ITER-like wall it is easier to operate at much higher pre-fill pressures than with the carbon wall (see figure 3). The dependency of the burn-through limit on electric field and pre-fill pressure can be added to the criteria for a successful avalanche. Interestingly, the model shows that even for pure deuterium plasmas, the maximum pre-fill is lower than the limit at which the avalanche would fail. Hence, at too high a pre-fill the breakdown would fail, not because the avalanche fails but first because it will not be able to burn-through. Note, that for the ITER-like wall much higher pre-fill pressures could be used than with the carbon wall.

CONCLUSIONS

A considerable effort has been initiated to improve the understanding of plasma breakdown in large tokamaks. The analysis presented in this paper attempts to provide a general experimental characterisation of both the avalanche as well as the burn-through phase of plasma breakdown at JET. It has also high lighted a number of issues that require further attention.

It was found that the avalanche phase at JET could be reasonably well described by a 0D Townsend model. The dependency on the density and current obtained as a function of the pre-fill clearly show the Townsend character of this phase. However, the comparison fails for some low voltage

breakdowns. The detailed dynamics of the initial plasma within the large vessel, its expansion but also its radial and vertical movement may have to be considered. It is also thought that the error field dynamics and the influence of eddy currents induced in the surrounding passive structures, become important and efforts are undertaken to model this more accurately [12, 13].

In general, failures in the avalanche phase are rare. For operation with the carbon wall only a small fraction (a few percent) failed in the avalanche phase, mainly due to too low or zero pre-fill pressure, while >85% of all non-sustained breakdown failures occurred in the burn-through phase. Mostly such events could be connected to deconditioning problems, for example after disruptions [18]. All other failures were due to technical problems, like an emergency shut-down of coil power supplies. For the period of carbon wall operations considered in the analysis (2008-2009), 8.8% of all discharges had a failed breakdown, while this dropped to 2.7% with the ITER-like wall. All most all were found to be due to technical issues while failures due to burn-through problems were nearly absent with the ITER-like wall (i.e. one case observed being a low voltage Mode B during a session with N seeding). With the ITER-like wall there was no need for glow discharge cleaning or beryllium evaporation to improve wall conditions to facilitate plasma initiation.

The ITER-like wall was found to have a profound impact on plasma breakdown. The avalanche phase was unaffected and seems to be dominated by the pre-fill pressure and its composition (i.e. type of gas). But as expected, the burn-through phase strongly depends on the plasma facing material. The highest radiation levels during the burn-through phase of ITER-like wall breakdowns were obtained at the start of operation, when the carbon levels were higher, but also during and after the use of N as extrinsic impurity. No clear trend was found with respect to the oxygen content of the plasma. The lower radiation efficiency of beryllium in comparison to carbon in combination with the fact the peak radiation is at lower temperature, allows for a faster burn-through. For the carbon wall, recycling and impurity sputtering were responsible for a large part of the electron density build up during the burn-through phase. In contrast, this component was absent with the ITER-like wall and also during the burn-through phase the density was determined by the amount of pre-fill gas making it more reproducible. The changes in breakdown with the ITER-like wall did not lead to a substantial reduction in flux-consumption.

With the ITER-like wall higher pre-fill pressures and higher densities during the burn-through phase could be achieved, though with significantly lower radiation. The lower recycling with the ITER-like wall also required additional pre-fill, fuelling and improved control and fuelling right after breakdown to maintain the density. It is possible that this effect complicates the low voltage breakdown (Mode B) at JET for which the Townsend avalanche criteria limit the pre-fill pressures range.

The analysis showed that it is possible to experimentally characterise both the avalanche and burn-through phase at JET in detail. The impact of the plasma-facing components on the burn-through phase is pronounced, as shown by the newly developed model. The analysis and modelling is been extended to take into account profile effects, as presently the model is merely 0D. Moreover, studies to improve the understanding of eddy currents on the error field dynamics on low voltage breakdown at JET are being planned.

ACKNOWLEDGEMENTS

This research was funded partly by the European Communities under the contract of Association between EURATOM and FOM and was carried out within the framework of the European Fusion Development Agreement. The views and opinions expressed herein do not necessarily reflect those of the European Commission.

REFERENCES

[1]. Sips, A.C.C., et al., Nuclear Fusion **49** (2009) 085015.
[2]. Lloyd, B., et al., Nuclear Fusion **31** (1991) 2031.
[3]. Lloyd, B., et al., Plasma Physics and Controlled Fusion **38** (1996) 1637.
[4]. Yoshino, R., et al., Plasma Physics and Controlled Fusion **39** (1997) 205.
[5]. Lazerus, E.A., et al., Nuclear Fusion **38** (1998) 1083
[6]. Philipps, V., et al., Fusion Enginering and Design **85** (2010) 1581.
[7]. Poploular, R., Nucl. Fusion **16** (1976) 37.
[8]. Tanga, A., et al., in Tokamak Start-up (Ed. H. Knoepfel) Plenum Press (1986) p159.
[9]. Valovic, M, et al., Nuclear Fusion **27** (1987) 599.
[10]. Jackson, G.L., et al., Nuclear Fusion **51** (2011) 083015.
[11]. Kim, H.T., Sips, A.C.C. and Fundamenski W, Nucl. Fusion **52** (2012) 103016
[12]. Maviglia, F., et al., Fusion Enginering and Design (2011) 675.
[13]. Albanese, R., et al., submitted to Nuclear Fusion (2012)
[14]. Brezinsek, S., et al., submitted Journal Nuclear Materials (2013)
[15]. Kim, H.T., Sips, A.C.C. and Fundamenski W., submitted to Journal Nuclear Materials (2013)
[16]. Giroud, C., et al., 25th IAEA Fusion Energy Conference (San Diego, 2012)
[17]. de Vries, P.C., et al., accepted in Plasma Physics and Controlled Fusion **54** (2012)

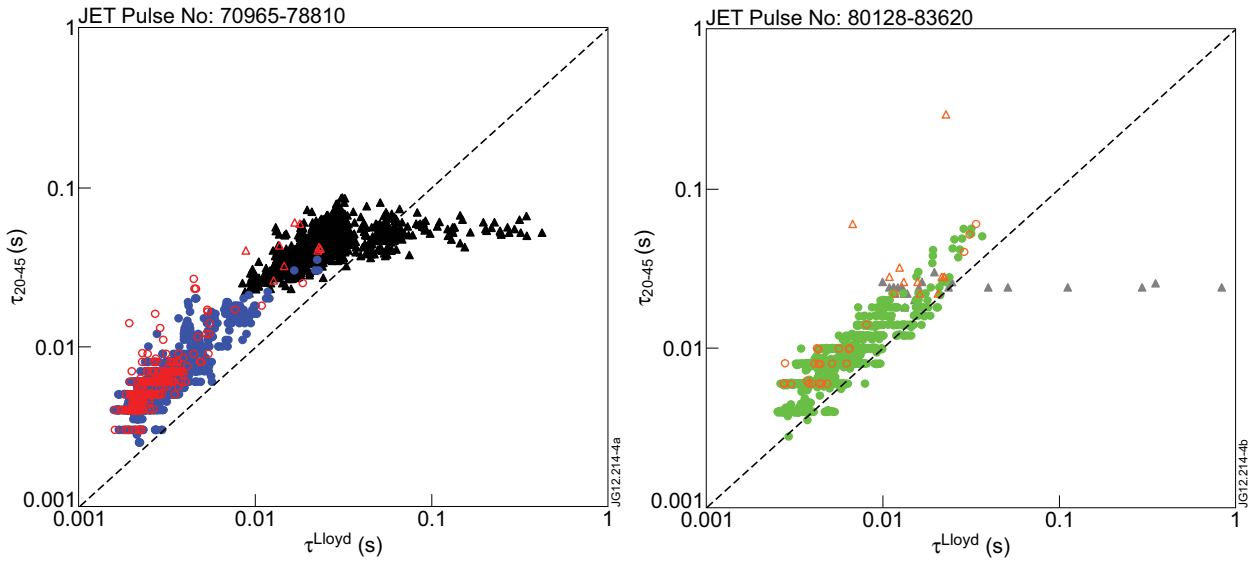

Figure 1: A comparison of the measured avalanche duration and that determined with equation 1 for a) carbon wall data and b) ITER-like wall data.

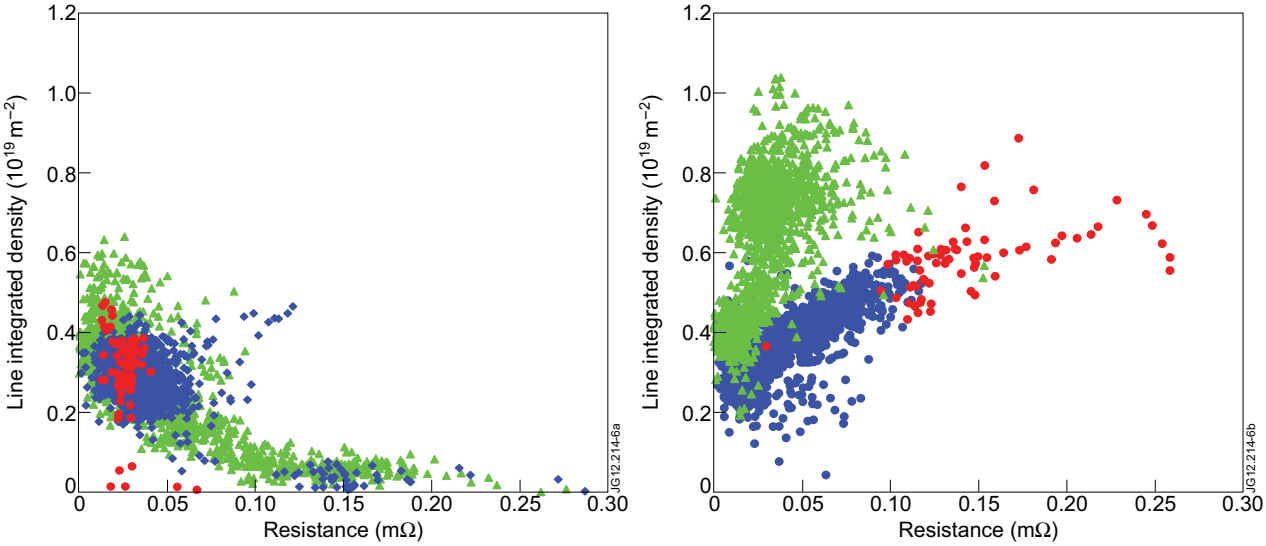

Figure 2: The line-integrated density as a function of the calculated plasma resistance using equation 2 at a) at t_1=0.031s and b) at t_2=0.051s.

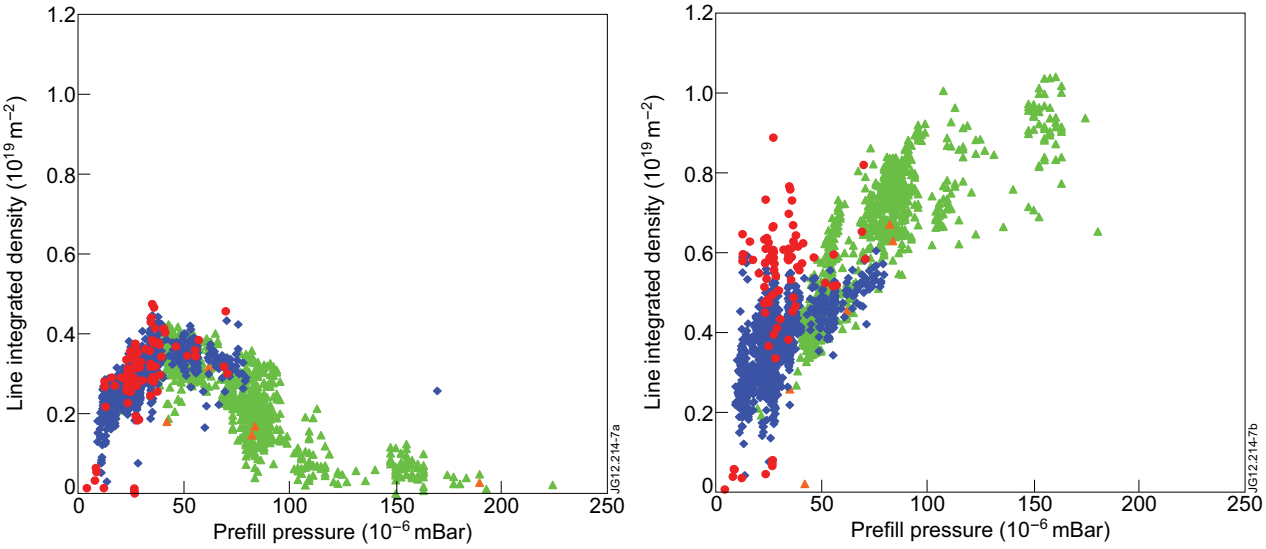

Figure 3: The line-integrated density as a function of the pre-fill pressure at a) at t_1=0.031s and b) at t_2=0.051s.

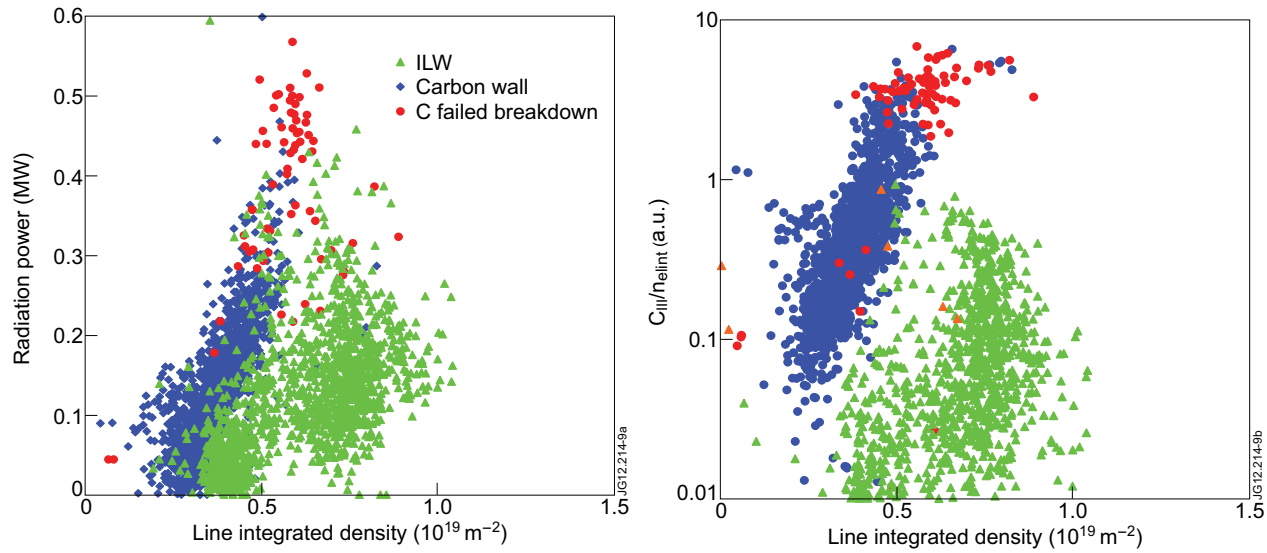

Figure 4: a) The radiation and b) carbon level (i.e. the CIII (λ_{CIII}=977Å) line-intensity, normalised to the density) versus the line-integrated density.